

# Large spot size and low-divergence angle operation of 917-nm edge-emitting semiconductor laser with an asymmetric waveguide structure

Jianxin Zhang (张建心)<sup>1</sup>, Lei Liu (刘磊)<sup>1</sup>, Wei Chen (陈微)<sup>1</sup>,  
Anjin Liu (刘安金)<sup>1</sup>, Wenjun Zhou (周文君)<sup>1</sup>, and Wanhua Zheng (郑婉华)<sup>1,2\*</sup>

<sup>1</sup>Nano-optoelectronics Laboratory, Institute of Semiconductors, Chinese Academy of Sciences, Beijing 100083, China

<sup>2</sup>State Key Laboratory on Integrated Optoelectronics, Institute of Semiconductors, Chinese Academy of Sciences, Beijing 100083, China

\*Corresponding author: whzheng@semi.ac.cn

Received October 25, 2011; accepted December 5, 2011; posted online February 20, 2012

GaInAs/AlGaAs comprehensive-strained three-quantum-well lasers with asymmetric waveguide are designed and optimized. With this design, the optical field in the transverse direction is extended, and a semiconductor laser with large spot is obtained. For a 300- $\mu\text{m}$  cavity length and 100- $\mu\text{m}$  aperture device under continuous wave (CW) operation, the measured vertical and horizontal far-field divergence angles are 12.2° and 3.0°, respectively. The slope efficiency is 0.44 W/A and the lasing wavelength is 917 nm. The equivalent transverse spot size is 3  $\mu\text{m}$  for the fundamental transverse mode, which is a sufficiently large value for the purpose of coupling and manipulation of light.

OCIS codes: 140.0140, 140.5960.

doi: 10.3788/COL201210.061401.

Large spot size enables small beam divergence of semiconductor lasers and increases the maximum attainable continuous wave (CW) output power. Smaller beam divergence makes direct coupling to optical fiber and for external cavity applications easier. At the same time, a high power to reach catastrophic optical mirror damage (COMD) make pumping the solid-state lasers, laser processing, and laser medical areas more attainable. In semiconductor lasers, the strong localization of the optical field in the transverse direction results in large far-field angle and lower maximum output power. These two disadvantages greatly restrict the application of semiconductor laser. Several approaches, such as ultrathin core-extended waveguide structure<sup>[1]</sup>, broad symmetric waveguide<sup>[2]</sup>, designs with mode-expansion layers<sup>[3–5]</sup>, and composite waveguides<sup>[6–8]</sup> have been proposed to enlarge spot size in edge-emitting lasers<sup>[9]</sup>. However, because these structures adopt symmetric waveguides, the optical field penetration into the p-type cladding layer enhances the free carrier absorption, which will significantly increase the internal loss of the laser. If the optical confinement factor ( $\Gamma$ -factor) is reduced further, the light loss will become more severe. One way to solve this problem is by using an asymmetric waveguide to change the distribution of the optical field. To realize this purpose, the asymmetric waveguide must be optimized to reduce the optical mode in p-type cladding layer by widely expanding the optical mode into the n-type cladding layer. With the asymmetric structure, a laser with large spot size and low internal loss could also be obtained<sup>[10–13]</sup>. Furthermore, asymmetric waveguide structures also permit higher doping of the p-type cladding layer to reduce resistance.

In this letter, we report on a large equivalent transverse spot size of 3  $\mu\text{m}$  for the fundamental transverse mode and a low vertical far-field angle of 12.2° using a

carefully designed asymmetric waveguide structure at a lasing wavelength of 917 nm. Thus far, a large equivalent transverse spot size and small vertical far-field angle has not yet been experimentally demonstrated using an asymmetric waveguide structure at this wavelength. Because the asymmetric laser structure reduces the internal loss of the laser, the threshold current can remain acceptably low<sup>[3]</sup>.

The complete semiconductor laser was epitaxially grown by low-pressure metal-organic chemical vapor deposition on a GaAs substrate, as shown in Table 1. The 4- $\mu\text{m}$ -thick Al<sub>0.25</sub>Ga<sub>0.75</sub>As as n-cladding layer was grown on a GaAs buffer layer. The n-SCH (SCH: separate confinements heterostructure) layer of 0.12- $\mu\text{m}$ -thick Al<sub>0.2</sub>Ga<sub>0.8</sub>As was grown on the n-cladding layer. The active region consists of three 7-nm-thick Ga<sub>0.92</sub>In<sub>0.08</sub>As quantum wells (QWs) separated by a 10-nm-thick Al<sub>0.1</sub>Ga<sub>0.9</sub>As barrier. The p-type layer consisted of a 0.12- $\mu\text{m}$ -thick Al<sub>0.2</sub>Ga<sub>0.8</sub>As SCH layer, a 1.4- $\mu\text{m}$ -thick Al<sub>0.4</sub>Ga<sub>0.6</sub>As cladding layer, and a 0.3- $\mu\text{m}$ -thick GaAs p-contact layer.

**Table 1. Structure of Designed Asymmetric Waveguide Laser Drawing in the Growth Direction**

p-GaAs Contact Layer: 0.2 $\mu\text{m}$	
p-Al <sub>0.4</sub> Ga <sub>0.6</sub> As Cladding Layer: 1.4 $\mu\text{m}$	
p-Al <sub>0.2</sub> Ga <sub>0.8</sub> As SCH Layer: 0.12 $\mu\text{m}$	
Al <sub>0.1</sub> Ga <sub>0.9</sub> As Barrier Layer: 0.01 $\mu\text{m}$	
MQW	Ga <sub>0.92</sub> In <sub>0.08</sub> As Well: 0.007 $\mu\text{m}$
	Al <sub>0.1</sub> Ga <sub>0.9</sub> As Barrier: 0.01 $\mu\text{m}$
n-Al <sub>0.2</sub> Ga <sub>0.8</sub> As SCH Layer: 0.12 $\mu\text{m}$	
n-Al <sub>0.25</sub> Ga <sub>0.75</sub> As Cladding Layer: 4.0 $\mu\text{m}$	
n-GaAs Buffer Layer: 0.3 $\mu\text{m}$	
n-GaAs Substrate	

The laser diode was fabricated using the standard semiconductor processes. First, a 100- $\mu\text{m}$ -wide ridge waveguide was fabricated by optical lithography and wet etching methods; a 250-nm-thick  $\text{SiO}_2$  layer was deposited on the whole wafer surface as the insulated layer; the  $\text{SiO}_2$  on top of the ridge was removed by secondary optical lithography and wet etching to ensure that the p-type contact layer was exposed; the Ti-Au metals were deposited on the p-type contact layer by an e-beam evaporator; after the substrate was lapped down to a thickness of 140  $\mu\text{m}$ , the AuGe-Ni-Au metals were thermally deposited onto the substrate. The device was mounted p-side down on a Cu mount using In solder material uncoated for high and anti reflection and attached to a thermoelectric cooler for testing<sup>[14,15]</sup>.

The refractive index is shown in Fig. 1. Shown as the dashed line, the fundamental transverse-mode intensity distribution  $\varphi^2(x)$  is normalized. The fractions of Al components in the two cladding layers are optimized. The Al component in the n-cladding layers is reduced, whereas the thickness is increased. The lower fraction of the Al component increases the refractive index of the n-type cladding layer, which makes the optical field leave the p-type material side, thereby reducing free-carrier absorption, scattering of light, and the internal loss of the high doped p-type cladding layer. The asymmetric refractive index distribution also expands the optical mode into the n-type cladding layer, and reduces the optical confinement factor  $\Gamma$ . Because the output power of semiconductor lasers is proportional to  $d/\Gamma$ , the so-called equivalent transverse spot size for a given optical power density value at COMD, where  $d$  is the active layer thickness and  $\Gamma$  is the optical confinement factor<sup>[16]</sup>. For the purpose of reducing the beam divergence and increasing the maximum attainable CW light output power from semiconductor lasers, equivalent transverse spot size is highly desirable.

Figure 2 shows the characteristics of the asymmetric waveguide laser with a cavity 300  $\mu\text{m}$  in length and a stripe 100- $\mu\text{m}$  wide at room temperature in the CW operation mode. Figure 2(a) shows the measured light output power, voltage versus current (L-I-V). Figure 2(b) shows the lasing spectrum. Figure 2(c) illustrates the differential resistance of the laser calculated by the voltage versus current curve from Fig. 2(a). Output power was measured as 100 mW, which was limited by the maximal measuring range of our equipment. Slope efficiency was measured as 0.44 W/A. Slope efficiency of the laser action satisfies the relation  $\eta \leq \alpha_m/(\alpha_m + \alpha)$ , where  $\alpha_m$

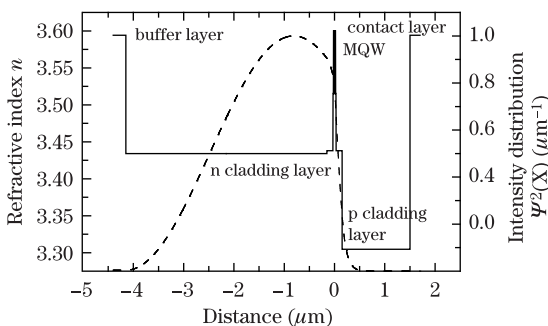


Fig. 1. Refractive index profile and intensity of fundamental transverse mode in the asymmetric laser structure.

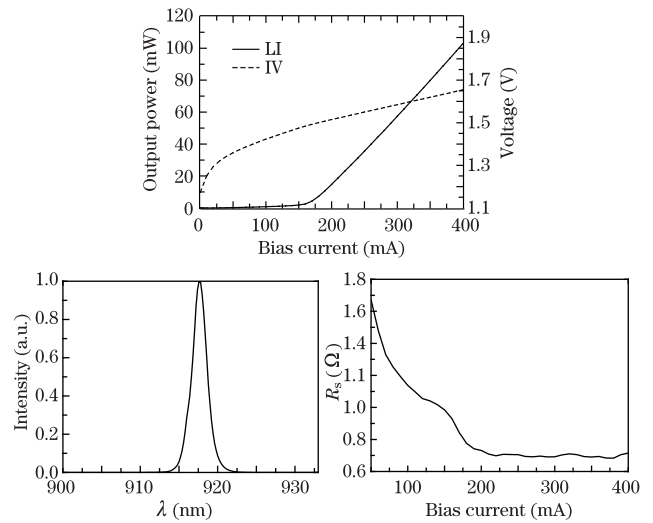


Fig. 2. Measured CW. (a) The light output power, voltage versus current (L-I-V); (b) the lasing spectrum at room temperature; (c) the calculated differential resistance of the laser.

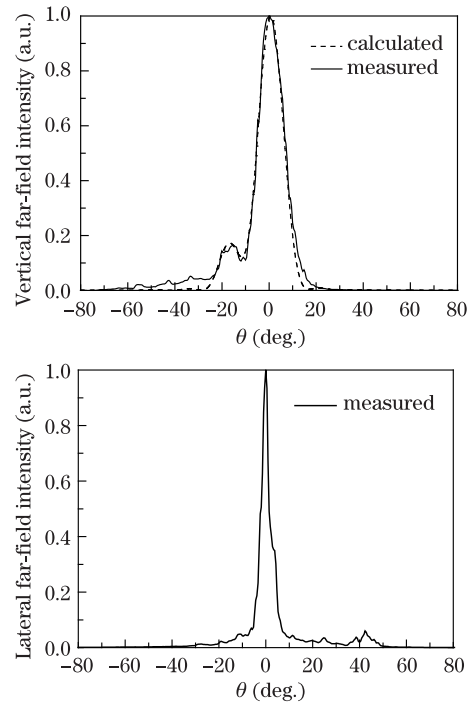


Fig. 3. (a) Vertical and (b) lateral far-field divergence angles at 300-mA injection current.

is mirror losses and  $\alpha_i$  is the internal loss. According to the equation,  $\alpha_i$  is the key parameter. Here,  $\alpha_i$  can be reduced by optimizing the doping profile and the optical field distribution<sup>[17,18]</sup>. By decreasing it, we can expand beam width further while preserving  $\eta$ . The threshold current was measured as 169 mA, and the corresponding threshold current density was measured as 563  $\text{A}/\text{cm}^2$  for the sample laser. The wavelength of the laser was measured as 917 nm, as shown in Fig. 2(b).

The vertical and lateral far-field divergence angles under 300-mA CW injection current are shown in Fig. 3. Although accompanied by a slight side lobe, an extremely narrow vertical far-field was obtained. The vertical far-field divergence angle was measured to be 12.2°. The-

oretically, the vertical far-field divergence angle of the designed structure can be obtained by

$$\psi(\theta) \propto \cos^2 \theta \left| \int_{-\infty}^{+\infty} \varphi(x) e^{ikx \sin \theta} dx \right|^2, \quad (1)$$

where  $\psi(\theta)$  is the intensity of the vertical far-field. From Eq. (1), for the given values of the thickness of the asymmetric waveguide, the vertical far-field divergence angle was calculated to be  $12.4^\circ$  at the emission wavelength. This value is consistent with the measured value in the experiment. The slight side lobe on the left of the main lobe is caused by the far-field of higher order transverse mode. Due to the expansion of the mode spot, the optical confinement factor of the fundamental transverse mode is reduced, which results in the lasing of higher order modes. However, the high-order modes are expected to experience a higher leaky loss than fundamental mode. Such leaky loss can be enhanced by reducing the ridge width or increase the etching depth<sup>[19]</sup>. Therefore, a single fundamental mode lasing is expected by designing appropriate ridged waveguide. We also need to make sure that the leaky loss is as small as possible to preserve the higher slope efficiency. According to Ref. [20], the etch depth can also affect the slope efficiency and have an optimal value. The dotted line in Fig. 3(a) is obtained by linear fitting of the far-fields of the fundamental and the first order transverse mode. The far-field of transverse modes deviate the normal direction of the facet, which is attributed to the deformation of the phase surface of each transverse mode, caused by the leaky loss to the substrate. As shown in the figure, the far-field intensity of the laser is mainly from the fundamental transverse mode in power range  $<100$  mW. We calculated the optical confinement factor of the fundamental transverse mode, and obtained the equivalent transverse spot size of  $d/\Gamma \approx 3 \mu\text{m}$ . This value is large for the purpose to couple and manipulate of light. Figure 3(b) shows the lateral far-field divergence angle of  $3^\circ$ .

In conclusion, we optimize asymmetric waveguide to maximize mode expansion and to reduce optical confinements across the waveguide. In our optimized structure, the width of n-type cladding layer set to  $4 \mu\text{m}$  will achieve a large equivalent transverse spot size and a low vertical far-field angle. As a result, a large equivalent transverse spot size of  $3 \mu\text{m}$  for the fundamental transverse mode, a small vertical far-field angle of  $12.2^\circ$ , and a slope efficiency of  $0.44 \text{ W/A}$  are measured mainly in CW operation from the uncoated  $300\text{-}\mu\text{m}$ -long asymmetric waveguide laser. We also confirm that using the asymmetric waveguide structure could be effective for obtaining large spot size and low vertical far-field angle laser.

This work was supported by the Chinese National Key Basic Research Special Fund/CNKBRSF (No.

2011CB922000), the National Natural Science Foundation of China (Nos. 61025025 and 60838003), and the National High Technology Research and Development Program of China (Nos. 2007AA03Z410 and 2007AA03Z408).

## References

1. T. Murakami, K. Ohtaki, H. Matsubara, T. Yamawaki, H. Saito, K. Isshiki, Y. Kokubo, A. Shima, H. Kumabe, and W. Susaki, *IEEE J. Quantum Electron.* **QE-23**, 712 (1987).
2. A. Al-Muhanna, L. J. Mawst, D. Botez, D. Z. Garbuzov, R. U. Martinelli, and J. C. Connolly, *Appl. Phys. Lett.* **73**, 1182 (1998).
3. G. Lin, S. Yen, and C. Lee, *IEEE Photon. Technol. Lett.* **8**, 1588 (1996).
4. G. Yang, G. M. Smith, M. K. Davis, A. Kussmaul, D. A. S. Loeber, M. H. Hu, H.-K. Nguyen, C.-E. Zah, and R. Bhat, *IEEE Photon. Technol. Lett.* **16**, 981 (2004).
5. T. Temmyo and M. Sugo, *Electron. Lett.* **31**, 642 (1995).
6. H. Wenzel, F. Bugge, G. Erbert, R. Hulsewede, R. Staske, and G. Trankle, *Electron. Lett.* **37**, 1024 (2001).
7. M. C. Wu, Y. K. Chen, M. Hong, J. P. Mannaerts, M. A. Chin, and A. M. Sergent, *Appl. Phys. Lett.* **59**, 1046 (1991).
8. Y. C. Chen, R. G. Waters, and R. J. Dalby, *Electron. Lett.* **26**, 1348 (1990).
9. M. V. Maximov, Y. M. Shernyakov, I. I. Novikov, L. Y. Karachinsky, N. Y. Gordeev, U. Ben-Ami, D. Bortman-Arbiv, A. Sharon, V. A. Shchukin, and N. N. Ledentsov, *IEEE J. Sel. Top. Quantum Electron.* **14**, 1113 (2008).
10. B. S. Ryvkin and E. A. Avrutin, *J. Appl. Phys.* **97**, 113106 (2005).
11. B. S. Ryvkin and E. A. Avrutin, *J. Appl. Phys.* **97**, 123103 (2005).
12. B. S. Ryvkin and E. A. Avrutin, *J. Appl. Phys.* **98**, 026107 (2005).
13. B. S. Ryvkin and E. A. Avrutin, *J. Appl. Phys.* **105**, 103107 (2009).
14. K. C. Kim, Il Ki Han, Y. C. Yoo, Jung Il Lee, Y. M. Sung, and T. G. Kim, *IEEE T. Nanotechnol.* **7**, 135 (2008).
15. K. C. Kim, D.-K. Jang, Jung Il Lee, T. G. Kim, W. W. Lee, J. H. Kim, E. J. Yang, B. J. Koo, and Il Ki Han, *IEEE Photon. Technol. Lett.* **21**, 1438 (2009).
16. D. Botez, *Appl. Phys. Lett.* **74**, 3102 (1999).
17. M. Levy, Y. Karni, N. Rapaport, Y. Don, Y. Berk, D. Yanson, and S. Cohen, *Proc. SPIE* **7583**, 75830J (2010).
18. Z. Xu, W. Gao, L. Cheng, K. Luo, K. Shen, and A. Mastrovito, *Proc. SPIE* **6909**, 69090Q (2008).
19. B. Corbett, P. Lambkin, J. O'Callaghan, S. Deubert, W. Kaiser, J. P. Reithmaier, and A. Forche, *IEEE Photon. Technol. Lett.* **19**, 916 (2007).
20. Y. Cao, "Al-free High Power and High Brightness Diode Lasers" (in Chinese) PhD. Thesis (Institute of Semiconductor Chinese Academy of Sciences, 2006).